J Mater Sci (2009) 44:6601–6607
DOI 10.1007/s10853-009-3611-8

MESOSTRUCTURED MATERIALS

Prussian Blue electrodeposition within an oriented mesoporous silica film: preliminary observations

Aurélie Goux · Jaafar Ghanbaja · Alain Walcarius

Received: 28 November 2008 / Accepted: 16 May 2009 / Published online: 2 June 2009

Abstract Prussian Blue (PB) has been electrochemically grown through thin mesoporous silica films of novel generation, exhibiting regular arrays of hexagonally packed mesopores channels (3 nm in diameter) oriented perpendicular to the underlying electrode surface. Due to confinement effects, special care has to be taken to ensure effective permeability of PB precursors through the hard silica template, which was best achieved by pulsed electrodeposition from a high ionic strength medium (2 M KCl). Energy dispersive X-ray spectroscopy associated to electron microscopy was used to evidence the presence of PB in the vertically-aligned mesopores, which was also assessed by their electrocatalytic behavior towards H_2O_2 reduction.

Introduction

Ordered porous thin films become increasingly exploited in electrochemistry [1]. Mesostructured silica-based materials are usually deposited as homogenous thin films onto flat supports by evaporation-induced self-assembly (EISA) of a surfactant-silicon alkoxide(s) mixture [2] and the permeability of mesoporous silica films on electrode surfaces is dependent on both the pore size and the mesostructure type [3–5]. We have recently discovered that electrochemistry provides a convenient way to prepare highly ordered mesoporous silica thin films with mesopore channels oriented perpendicularly to the underlying electrode [6], i.e., an "ideal" configuration for many applications, which remains very difficult to get by EISA [2, 7]. Here, such high-tech films are evaluated as possible hard template to electrodeposit Prussian Blue (PB) through a very high density of mesopore channels.

Prussian Blue (PB) derivatives represent an important class of mixed-valence compounds, which are among the most widely used mediators in electrochemical sensing and biosensing (see some representative reviews [8–10] and references cited therein). Recently, particular attention was given to nanostructuration of PB as this has proven to dramatically increase its analytical performance, notably the electrocatalytic detection of hydrogen peroxide [11, 12]. PB nanostructures are mostly manufactured in the form of nanotube or nanowire arrays, via electrodeposition through polycarbonate [13, 14] or porous alumina [15, 16] membranes, with sizes restricted to the 50–200 nm range. PB nanoparticles can be also prepared but they need to be stabilized by polymers for practical use in sensors [17]. An elegant method relies on PB electrodeposition using colloidal crystals (e.g., polystyrene beads [18]) or lyotropic liquid crystalline [11] or alkoxysilane sols [12] as sacrificial templates to generate continuous porous films.

Here, we have thus evaluated the possibility to generate PB nano-objects through an oriented mesoporous silica matrix previously formed on ITO electrode, which pore diameter (ca. 3 nm) much smaller than the polymer or ceramic membranes. After optimization of the electrodeposition parameters, the presence of PB will be pointed out by physico-chemical and electrochemical methods, and its electrocatalytic behavior will be tested for H_2O_2 detection.

A. Goux · A. Walcarius (✉)
Laboratoire de Chimie Physique et Microbiologie pour l'Environnement, UMR 7564—CNRS—Nancy-Université, 405, rue de Vandœuvre, 54600 Villers-lès-Nancy, France
e-mail: alain.walcarius@lcpme.cnrs-nancy.fr

J. Ghanbaja
Service commun de microscopies électroniques et microanalyses X—Faculté des Sciences, Nancy-Université, BP 239, Boulevard des Aiguillettes, 54506 Vandœuvre-lès-Nancy Cedex, France

Experimental

Mesoporous silica thin films preparation

Oriented mesoporous silica films were potentiostatically deposited (−1.3 V for 20 s) onto ITO plates (surface resistivity = 8–12 Ω, Delta Technologies), onto a surface area of 0.50 cm^2. This was made as previously described [6, 19], from a precursor sol consisting in 20 mL ethanol (95–96%, Merck), 20 mL aqueous solution of 0.1 M $NaNO_3$ (99%, Fluka) and 0.1 M HCl (37%, Riedel de Haen) to which 75 mM tetraethoxysilane (TEOS, 98%, Alfa Aesar) and 24 mM cetyltrimethylammonium bromide (CTAB, 99%, Acros) were added under stirring. The electrode was quickly removed from the solution and immediately rinsed with distilled water and the deposit was dried and aged overnight in an oven at 130 °C. Extraction of the surfactant was achieved by calcination at 450 °C for 30 min (effectiveness of template removal was checked by IR spectroscopy).

Prussian Blue electrodeposition

Three electrochemical methods have been used to prepare PB deposits: cyclic voltammetry (CV), chronoamperometry (CA), and pulsed chronoamperometry. Typical solutions contained 4 mM $K_3Fe(CN)_6$ (analytical grade, Fluka), 4 mM $FeCl_3 \cdot 6H_2O$ (analytical grade, Fluka), 0.1 M HCl and KCl (99%, Prolabo) at concentrations ranging from 0.1 to 4 M. CV synthesis consisted in potentiodynamic cycling between +0.3 and +0.8 V (at 40 mV s^{-1}). Electrodeposition of PB by CA or pulsed CA consisted in applying +0.35 V for a given period of time or pulses at +0.35 V and +0.55 V for defined lapses of time, respectively. The silica film was immersed in the electrodeposition solution 15 min before applying potentials. After deposition, PB was electrochemically activated in 0.1 M HCl and 0.1 M KCl by CV from −0.05 to 0.35 V (at 40 mV s^{-1}) until reaching a stable voltammogram. H_2O_2 (35%, Carlo Erba) detection was performed by CV in phosphate buffer (pH 6).

Instrumentation

Mesoporous silica films and PB deposits were characterized by transmission electron microscopy (TEM) using a Philips CM20 microscope at an acceleration voltage of 200 kV coupled with an energy dispersive X-ray (EDX) spectrometer. Line scans (0.7 μm length; 10 nm point spacing) were recorded for quantitative analysis of Fe, Si, and In elements. Samples were supported on a carbon-coated copper grid after mechanical removing from the electrode. Field-emission scanning electron microscopy (FE-SEM) was carried out using a Stereoscan 440 SEM apparatus (LEICA) having a 4.5-nm resolution and grazing-incidence X-ray diffraction (GIXD) was performed using a Nonius Kappa—CCD diffractometer equipped with an ApexII CCD detector (copper cathode (λ_{K_α} = 1.54184Å).

All electrochemical measurements were performed at room temperature with an Autolab PGSTAT-12 potentiostat (Eco Chemie) monitored by General Purpose Electrochemical System Software. Experiments were carried out in a three-electrode cell using ITO as working electrode, a silver/silver chloride reference electrode and stainless steel as counter-electrode.

Results and discussion

PB deposition on bare ITO electrode

Several tens of papers are published in the literature dealing with PB electrodeposition on various electrode surfaces (see [8–10] and Refs. therein), including some using ITO [20–25] even if this material is not the most common substrate for PB electrosynthesis. No information is, however, available on getting very thin (<50 nm, i.e., the order of magnitude of thickness of silica films) PB films in a controlled way so that deposition procedures were first investigated on bare electrode. Most conclusions are drawn from Fig. 1A–D. Typical deposition method is CV (Fig. 1A), involving the two redox systems: Berlin Green-PB at +0.78 V and PB-Prussian White at +0.5 V [26]. Figure 1B illustrates the electrochemical activation step after medium exchange to HCl/KCl solution, giving rise to characteristic peaks centered at +0.18 V corresponding to the Fe^{III}/Fe^{II} redox couple (Eq. 1) [27].

$$Fe_4^{III}[Fe^{II}(CN)_6]_3 + 4K^+ + 4e^- \Leftrightarrow K_4Fe_4^{II}[Fe^{II}(CN)_6]_3 \quad (1)$$

The shape of CV curves and location of voltammetric peaks are in good agreement with previous observations for PB on ITO [20, 25], the large difference in anodic-to-cathodic peak potentials being ascribed to both uncompensated ohmic drop and slow electron transfer processes [20]. These are due to surface-confined redox active species as their intensity was found to vary linearly with scan rate (in the range studied here: 20–100 mV s^{-1}). Film thickness can be estimated from integration of these signals according to Eq. 2 [20]:

$$l = \frac{Q}{nFA}\frac{d^3 N_A}{4} \quad (2)$$

where Q is the electrical charge obtained from voltammograms (Fig. 1B), A the electrode area, F the Faraday constant, n the number of electrons in the redox process, d

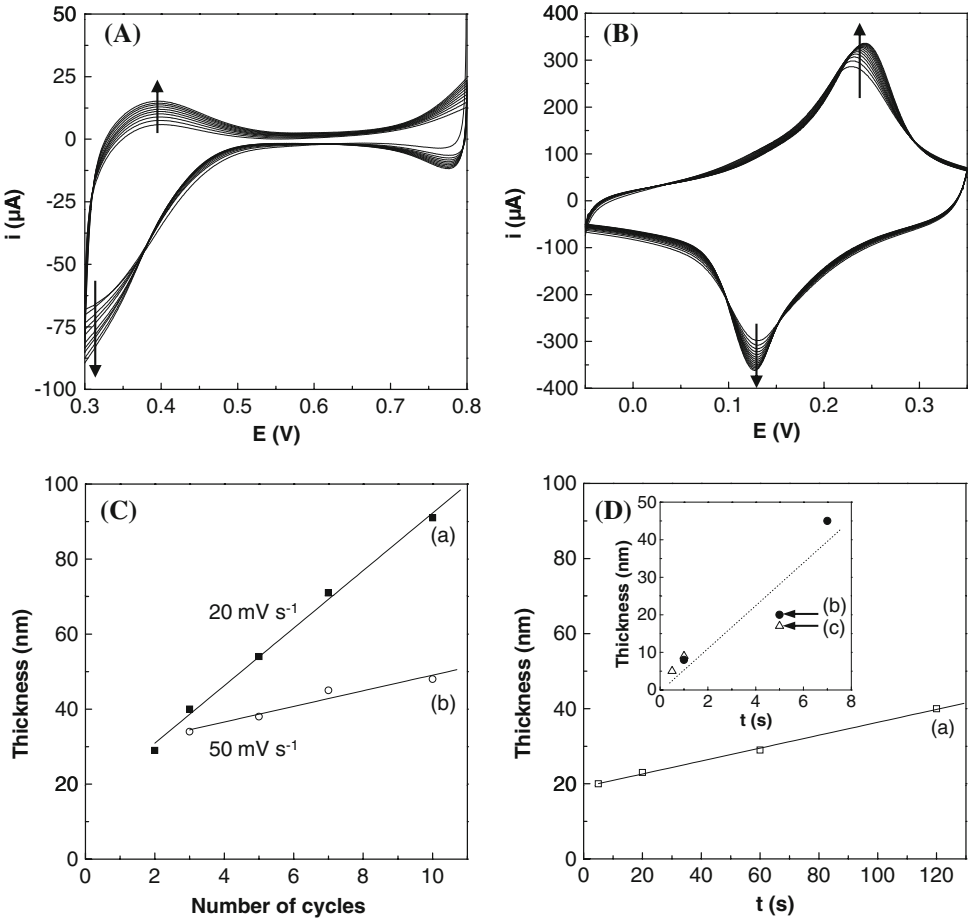

Fig. 1 **A** Electrodeposition of PB on ITO electrode (scan rate 40 mV s^{-1}) from 4 mM $K_3Fe(CN)_6$, 4 mM $FeCl_3$, 0.1 M HCl and 0.1 M KCl. **B** Activation of the PB film (scan rate 40 mV s^{-1}) in 0.1 M HCl and 0.1 M KCl. **C** and **D** Variation of the calculated thickness of PB films deposited by cyclic voltammetry at two different scan rates, 20 mV s^{-1} (*solid square*) and 50 mV s^{-1} (*open circle*), as a function of the number of cycles (**C**) and by chronoamperometry at +0.35 V (**D**) and pulsed chronoamperometry (inset in **D**) with two different pulse duration, 1 ms at +0.35 V and 10 ms at +0.55 V (*open triangle*) and 10 ms at +0.35 V and 100 ms at +0.55 V (*solid circle*), as a function of deposition time (**D**)

the length of the unit cell containing four iron atoms (10.17 Å) and N_A, is Avogadro's number.

Typical results (Fig. 1C) indicate a linear relation between film thickness and the number of cycles as well as faster growth when decreasing the potential scan rates (i.e., 8 and 2 nm/cycle at, respectively, 20 and 50 mV s^{-1}). This method operates quite well but does not allow preparing very thin films (<20 nm) as high potential scan rates and small number of cycles did not result in good PB films. A potential step (CA) was then applied, giving rise to film thickness increasing linearly with the deposition time, with a lower limit again at about 20 nm (Fig. 1D). The best results were obtained by pulsed CA, which permitted to control more accurately the electrodeposition process at short synthesis times. This gave rise to thin films growing linearly with deposition time in a thickness region down to 5 nm (see inset in Fig. 1D), independently on the pulse duration (1 or 10 ms, compare parts b, c).

PB deposition through mesoporous silica

Electro-assisted self-assembly (EASA) is a powerful and versatile method to produce crack-free mesoporous silica films exhibiting regular arrays mesopore channels oriented perpendicular to the underlying electrode surface [6, 19, 28]. Some physico-chemical characteristics of the films used here are illustrated in Fig. 2; they do not provide novel information with respect to previous reports [6, 19], but they are shown here to prove the good quality of the hard template then used for PB electrodeposition. The FE-SEM image (part A in Fig. 2) shows the uniformity of the deposit while TEM views (top and cross-sectional, see parts B and C in Fig. 2) point out the high level of ordering of hexagonally-packed mesopores normal to the ITO substrate. Part d of the figure confirms the existence of the highly ordered and oriented hexagonal mesostructure as GIXD pattern exhibits well-defined diffraction spots in the equatorial plane, which can be indexed to (11), (20) and (21) signals of a hexagonal lattice with a parameter of 40.7(±0.2) Å. The absence of cracks was demonstrated by cyclic voltammetry (see part E in Fig. 2) as no signal for a solution-phase redox probe ($[Ru(bpy)_3]^{2+}$) can be detected prior to removal of the surfactant template (curve b + inset) whereas a nice CV response was obtained after template extraction (curve c) which was even more intense than on bare ITO (curve a) as a result of favorable electrostatic interaction of the

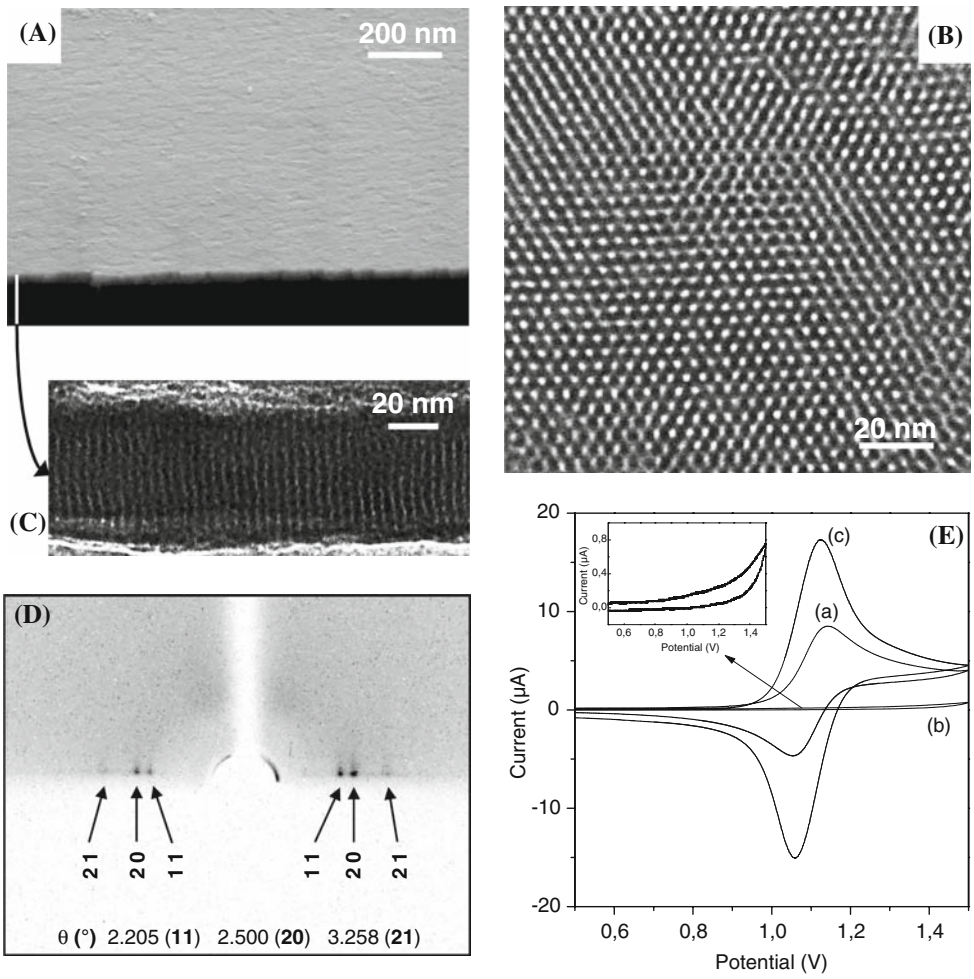

Fig. 2 **A** FE-SEM image, **B** top view TEM, **C** cross-sectional view TEM, and **D** GIXD pattern of a template-extracted mesoporous silica film which has been electrogenerated on ITO. **E** Cyclic voltammograms recorded in 0.5 mM $[Ru(bpy)_3]^{2+}$ at (a) bare ITO and at ITO electrodes covered with the mesoporous silica thin film, (b) prior to and (c) after surfactant extraction (inset: enlargement of curve b)

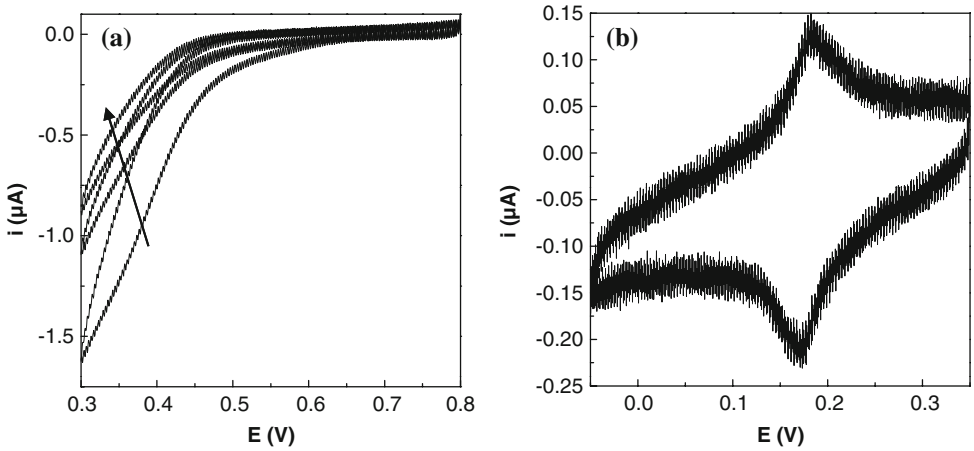

Fig. 3 **a** Electrodeposition of PB through a mesoporous silica-modified ITO electrode (scan rate 40 mV s^{-1}) from 4 mM $K_3Fe(CN)_6$, 4 mM $FeCl_3$, 0.1 M HCl and 0.1 M KCl and **b** activation of the PB film (scan rate 40 mV s^{-1}) in 0.1 M HCl and 0.1 M KCl

positively-charged probe with the negatively charged silica surface. These results are also indicative of the effectiveness of the surfactant extraction procedure.

PB deposition was thus made through such highly ordered and oriented mesoporous silica films on ITO (this substrate has been used as it ensures strong adhesion of the film to the electrode surface), first by applying the CV electrodeposition method. Comparing CV curves in part a of Fig. 1 and part a of Fig. 3 clearly indicate dramatic decrease in peak currents in the presence of the film on ITO. Also, the electrochemical activation (Fig. 3b) confirms the presence of electrodeposited PB, but in much

lower quantity as on bare ITO. No improvement was observed when applying CA or pulsed CA instead of CV for PB electrodeposition. The reason is probably a resistance to mass transport through the film, which was, however, not observed with $[Ru(bpy)_3]^{2+}$ probe but could occur with negatively charged redox species as $Fe(CN)_6^{3-}$, as reported for other mesoporous silica films deposited on electrode surfaces [4].

This was assessed by CV experiments (Fig. 4). Part A of the figure confirms that the film is homogeneously deposited over the entire ITO surface as it is totally impermeable to redox probes prior to surfactant extraction (see curve b), as previously discussed (Fig. 2E). After template removal, the film becomes permeable to $Fe(CN)_6^{3-}$ species, but the CV response remains dramatically lower than on bare ITO (compare curves c and a in Fig. 4A). This restriction can be attributed to unfavorable electrostatic interactions between the negatively-charged mesopore walls and $Fe(CN)_6^{3-}$ anions in such a confined environment [4]. It is thus necessary to control the charge selective behavior of the film by altering the ionic strength of the medium (Donnan exclusion behavior, as previously reported for templated polymer films [29]). Figure 4B shows that increasing the supporting electrolyte concentration contributes indeed to increasing significantly the permeability of the mesoporous silica film to $Fe(CN)_6^{3-}$ anions. Two molar KCl was chosen as the best compromise between sufficiently fast mass transport and long-term stability of the PB electrodeposition solution. Also, too long bathing of the mesoporous film in such highly ionic solution has to be avoided: it was checked by GIXD that the mesostructure was kept after ca. 2 min (i.e., less than the PB synthesis time) stay in 2 M KCl solution (similar GIXD pattern as in Fig. 2D), whereas significant loss in the ordered structure was observed after 2 h bathing in the same medium (disappearance of diffraction spots and presence of ill-defined ring on the GIXD pattern).

After checking that such change in ionic strength does not affect PB deposition on ITO, this medium was applied to generate PB through the mesoporous silica matrix on the electrode surface, respectively, by CV, CA and pulsed CA. This later gave the best results probably because the delay between each pulse is likely to favor re-equilibration of reagent concentrations in the restricted environment of mesopore channels. The CV activation curve (Fig. 5a) confirms the successful generation of PB by pulse CA on ITO through the mesoporous film and points out the beneficial effect of high ionic strength as CV signals are more than one order of magnitude larger than previously (Fig. 3b). The difference between anodic and cathodic peak potentials (10 mV, Fig. 5a) was much less than the bulk PB film (100 mV, Fig. 1B), arguing in favor of nanoscale deposits (values of 40 mV [14] and 20 mV [30] have been reported for PB nanowires of 200 and 50 nm sizes, respectively). Considering the measured electrical charge under the voltammetric signal (2.5 μC) and the effective iron atoms in the PB unit cell (4), data of Fig. 5a indicate that about 4×10^{12} unit cells of electroactive PB have been formed. Comparing this number to the number of mesopore channels present onto the ITO surface (about 2×10^{12} on the 0.5 cm^2 area sampled here), and assuming all mesopores likely to be filled (which is probably an overestimation), suggest that only 2 PB unit cells have been generated per mesopore. This is not that much, probably because the mesopore diameter (3 nm) is only a small multiple of the primitive cubic cell dimensions for PB (1.02 nm) and/or due to electrostatic repulsions of negatively charged PB precursors and the negatively charged silica surface, which is known to induce severe restrictions in the confined environment of long mesopore channels [31]. Attempts to increase the amount of deposited PB failed, presumably because of these restrictions (resistance to mass transport due to unfavorable electrostatic interactions). This suggests on the one hand that PB

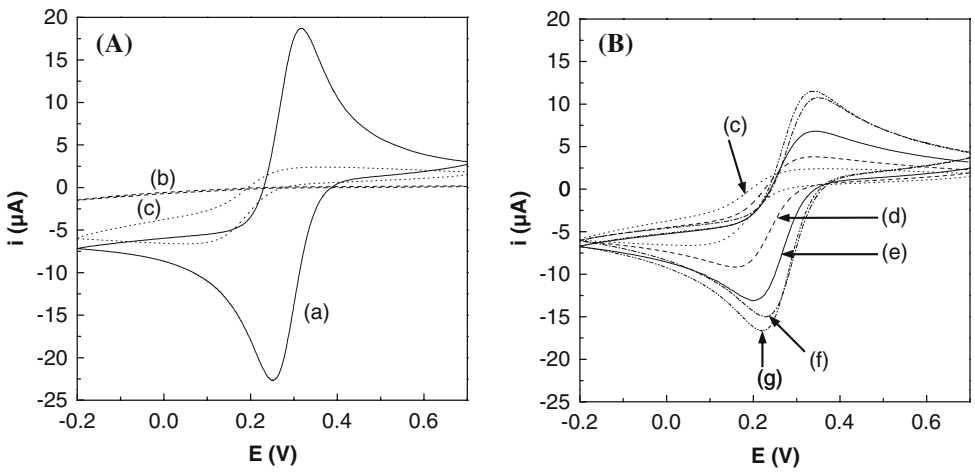

Fig. 4 **A** Cyclic voltammograms recorded in 0.1 M KCl solutions containing 0.5 mM $K_3Fe(CN)_6$ using a bare ITO electrode (a) or an ITO electrode covered with a mesoporous silica thin film (b) before and (c) after template extraction. **B** Cyclic voltammograms recorded as in (c) in part **A** of the figure, but in solutions containing 0.5 mM $K_3Fe(CN)_6$ and increasing KCl concentrations: 0.1 M (c), 1 M (d), 2 M (e), 3 M (f) and 4 M (g)

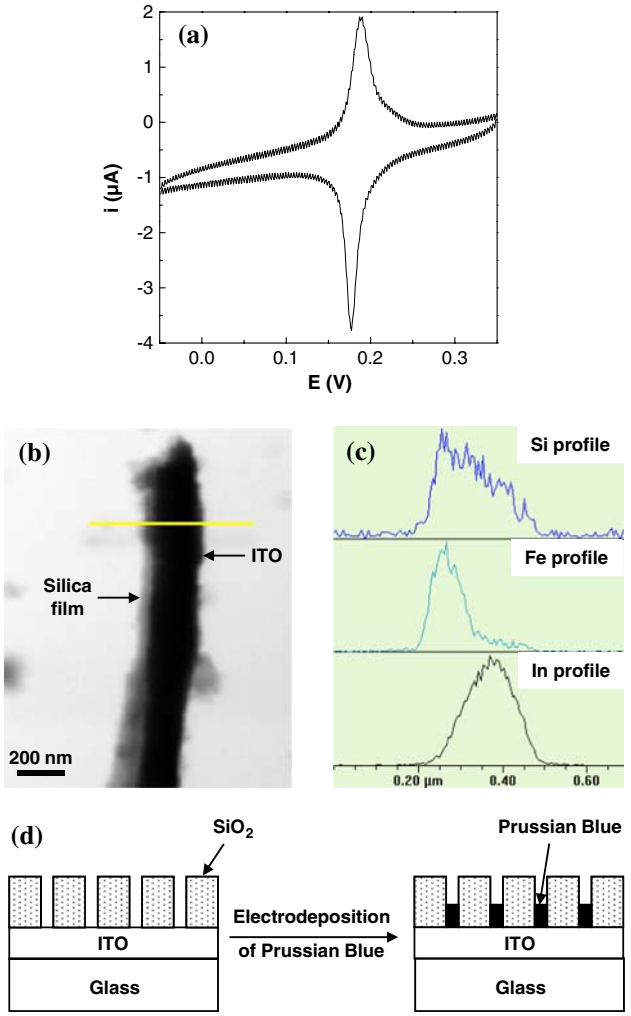

Fig. 5 **a** Cyclic voltammogram (scan rate 40 mV s^{-1}) recorded in 0.1 M HCl and 0.1 M KCl using the PB nanowires prepared by pulsed chronoamperometry within the mesoporous silica matrix; experimental deposition parameters: 10 ms at +0.35 V and 100 ms at +0.55 V (whole deposition duration at +0.35 V = 5 s) from a solution containing 4 mM $K_3Fe(CN)_6$, 4 mM $FeCl_3$, 0.1 M HCl and 2 M KCl. **b** Back-scattered electrons cross-sectional view of a piece of mesoporous silica/Prussian Blue film on ITO substrate. **c** Line scans recorded for quantitative analyses of silicon, iron, and indium, along the gray line depicted on part (**b**) of the figure. **d** Simplified scheme of electrodeposition of PB within the oriented mesoporous silica matrix

was not generated at defects places (otherwise PB would has continue to grow, including above the silica film) and, on the other hand, that nano-objects generation in so confined areas is not easy and one cannot state at this stage that nanowires have been formed but PB is indeed present on the electrode surface.

Direct observation of so small nano-objects in silica mesochannels is not straightforward, especially because the film is strongly adhesive to ITO and it has to be removed from the electrode surface to be imaged by TEM. Indeed, the film has undergone some damage upon pulling out and the cross-sectional view (Fig. 5b) does not allow identifying PB nano-objects, probably because of lack of contrast between silica and PB or too short wire length. Anyway, in spite of poor regularity of the observed sample (i.e., some part of the silica film are folded back to the ITO part), multi-element EDX analysis along the line depicted on Fig. 5b indicates from Si, Fe, and In profiles (Fig. 5c) that PB is mainly situated in the mesoporous silica film close to the ITO surface (Fe profile superimposes to the Si one but not to the In one). This suggests that PB is really formed within mesopores (Fig. 5d) and not within eventual cracks (yet not evidenced), which is also supported by the fact that no PB overlayer on the mesoporous silica film template was never observed when attempting to get thicker deposits. The amount of deposited PB was also too small to enable XRD characterization.

Response to H_2O_2

Some preliminary experiments have been performed to compare the electrocatalytic behavior of a bulk PB film-modified ITO (Fig. 6A) and PB nano-objects in mesoporous silica-modified ITO (Fig. 6B). In both plots, the curve "a" was registered in a blank buffered solution, and curves "b" and "c" in the presence of 10^{-4} and 10^{-2} M H_2O_2, respectively. Even if no attempt to optimize H_2O_2 detection has been made, these data indicate better electrocatalytic signal-to-background ratios for PB nanostructures in the silica matrix (see much bigger ratios between cathodic currents of curves "c" and "a" in part b than in part a of Fig. 6). Such enhancement appears rather overwhelming when considering that the amount of PB deposited in the mesochannels is lower by more than two orders of magnitude as in the bulk PB film. However, the particular shape of CV curves (linear increase in current for H_2O_2 reduction beyond 0.2 V, see Fig. 6B, as observed independently on scan rate in the 20–100 mV s^{-1} range) suggests either high resistance or some other significant limitation that might be due to the aforementioned restrictions in confined mesopores but no clear explanation is available at this stage. Also, the sensitivity to H_2O_2 remained much higher for the bulk PB film deposited on ITO (22 mA cm^{-2} M^{-1} in the H_2O_2 concentration range between 0.1 and 1.0 mM) in comparison to that observed with PB generated through the mesoporous silica film on the same geometric surface area (5 mA cm^{-2} M^{-1}). This effect can be also related to the dramatic difference in the measured currents on both types of PB deposits (Fig. 6), indicating that the electroactive PB area is ca. 1–2 orders of magnitude lower than the geometric surface area of the modified electrode, which suggests that a limited number of mesopore channels really incorporate PB nano-objects.

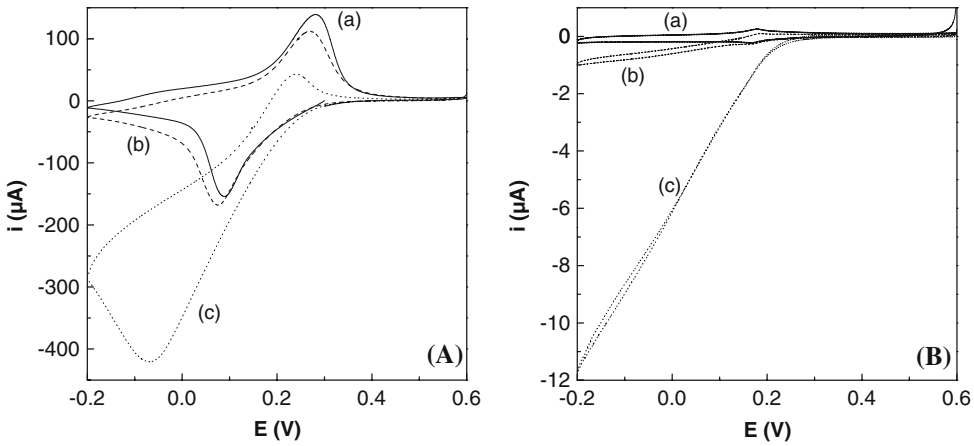

Fig. 6 Cyclic voltammograms recorded at 50 mV s^{-1} in phosphate buffer (pH 6) in the absence of H_2O_2 (a), or in the presence of (b) 0.1 mM or (c) 10 mM H_2O_2 using (**A**) a bulk PB film directly deposited on ITO or (**B**) PB nanowires deposited within an oriented mesoporous silica matrix previously electrogenerated onto the electrode surface

Conclusion

This work demonstrates that PB can be deposited through dense mesochannels of very small dimension (3 nm) but also that generation of nano-objects in a so confined medium suffers from strong restrictions as only a very small part of the pore volume can be filled. In spite of low amounts of deposited PB, their electrocatalytic properties towards reduction of H_2O_2 were maintained. This opens the way to the preparation of other oriented nano-objects (e.g., metal deposits) via nanocasting in electrogenerated mesoporous silica films.

Acknowledgements Financial supports from the French National Research Agency (project No NT05-3_41602 "mesoporelect") and Nancy University (BQR) are greatly appreciated. We are also grateful to S. Borensztajn for FE-SEM experiments and to E. Aubert for GIXD measurements. We thank the Service Commun de Diffraction X, Institut Jean Barriol—Nancy-Université, for providing access to crystallographic facilities.

References

1. Walcarius A, Kuhn A (2008) Trends Anal Chem 27:593
2. Sanchez C, Boissière C, Grosso D, Laberty C, Nicole L (2008) Chem Mater 20:682
3. Wei TC, Hillhouse HW (2007) Langmuir 23:5689
4. Etienne M, Quach A, Grosso D, Nicole L, Sanchez C, Walcarius A (2007) Chem Mater 19:844
5. Sel O, Sallard S, Brezesinski T, Rathousky J, Dunphy DR, Collord A, Smarsly BM (2007) Adv Funct Mater 17:3241
6. Walcarius A, Sibottier E, Etienne M, Ghanbaja J (2007) Nat Mater 6:602
7. Brinker CJ, Dunphy DR (2006) Curr Opin Colloid Interface Sci 11:126
8. Karyakin AA (2001) Electroanalysis 13:813
9. Koncki R (2002) Crit Rev Anal Chem 32:79
10. Ricci F, Palleschi G (2005) Biosens Bioelectron 21:389
11. Karyakin AA, Puganova EA, Budashov IA, Kurochkin IN, Karyakina EE, Levchenko VA, Matveyenko VN, Varfolomeyev SD (2004) Anal Chem 76:474
12. Karyakin AA, Puganova EA, Bolshakov IA, Karyakina EE (2007) Angew Chem Int Ed 46:7678
13. Ravindran S, Singh KV, Andavan GTS, Ozkan M, Gao Y, Hu E, Ozkan CS (2006) Nanotechnology 17:714
14. Qu F, Shi A, Yang M, Jiang J, Shen G, Yu R (2007) Anal Chim Acta 605:28
15. Johansson A, Widenkvist E, Lu J, Boman M, Jansson U (2005) Nano Lett 5:1603
16. Xian Y, Hu Y, Liu F, Xian Y, Feng L, Jin L (2007) Biosens Bioelectron 22:2827
17. Hornok V, Dekany I (2007) J Colloid Interface Sci 309:176
18. Qiu JD, Peng HZ, Liang RP, Xiong M (2007) Electroanalysis 19:1201
19. Goux A, Etienne M, Aubert E, Lecomte C, Ghanbaja J, Walcarius A (2009) Chem Mater 21:731
20. García-Jareño JJ, Navarro JJ, Roig AF, Scholl H, Vicente F (1995) Electrochim Acta 40:1113
21. Guo Y, Guadalupe AR, Resto O, Fonseca LF, Weisz SZ (1999) Chem Mater 11:135
22. Ho KC, Chen CY, Hsu HC, Chen LC, Shiesh SC, Lin XZ (2004) Biosens Bioelectron 20:3
23. Fiorito PA, Gonçales VR, Ponzio EA, Cordoba de Torresi SI (2005) Chem Commun 366
24. Yi IJ, Kim JH, Choi YJ, Kang CJ, Kim YS (2006) Microelectron Eng 83:1594
25. Shan Y, Yang G, Gong J, Zhang X, Zhu L, Qu L (2008) Electrochim Acta 53:7751
26. Ellis D, Eckhoff M, Neff VD (1981) J Phys Chem 85:1225
27. Itaya K, Ataka T, Uchida I, Toshima S (1982) J Am Chem Soc 104:4767
28. Etienne M, Goux A, Sibottier E, Walcarius A (2009) J Nanosci Nanotechnol 9:2398
29. Elliot JM, Cabuché LM, Bartlett PN (2001) Anal Chem 73:2855
30. Liu SQ, Xu JJ, Chen HY (2002) Electrochem Commun 4:421
31. Amatore C, Oleinick A, Klymenko O, Delacôte C, Walcarius A, Svir I (2008) Anal Chem 80:3229